An Improved Functional Link Architecture for Nonlinear AEC

Srikanth Burra*, Asutosh Kar*, Mads Græsbøll Christensen†
*Indian Institute of Information Technology Design and Manufacturing, Chennai 600127, India.
†Audio Analysis Lab, Department of Architecture, Design and Media Technology, Aalborg University, Denmark.

***Abstract*—In practice, hands-free devices commonly employ low-cost electronic components. Unfortunately, the nonlinear distortion arising from them affects the performance of acoustic echo cancellers. To address this issue, this paper proposes a new adaptive filtering algorithm based on nonlinear acoustic echo cancellation (NAEC) framework for improving its echo cancellation performance. The advanced method employs a novel combination of an adaptive filter based on sub-filter and proportionate adaptation, and presents an enhanced NAEC framework. In addition to that, both convergence and steady-state analysis of the proposed NAEC algorithm are presented. The performance evaluation made in the presence of speech and colored noise inputs has shown an average improvement of 3-4 dB compared to the existing algorithms.**

***Index Terms*—Adaptive filtering, nonlinear acoustic echo cancellation, functional link adaptive filtering, echo return loss enhancement.**

I. Introduction

The nonlinear distortion (NLD) generated by the low cost loudspeakers, amplifiers in the hands-free devices will introduce nonlinearity in the acoustic path between loudspeaker and the microphone [1]. This hampers the job of acoustic echo cancellation (AEC) framework in estimating the room impulse response (RIR) of the acoustic echo path. As a result, the echo cancellation performance of AEC is reduced. Hence nonlinear AEC (AEC) algorithms based on state-space models [1], kernel methods [2] were reported in the literature to mitigate the effects of NLD on AEC in the RIR estimation. Similarly a nonlinear post-processor based NAEC was proposed in [3] to minimize the impact of NLD. As the name suggests, these algorithms employ a nonlinear filter to cancel the NLD at the output of AEC which can be used only for lower degree of NLD. In addition to these NAEC methods, the functional link (FL) based NAEC were proposed in [4], [5], [6] as a relatively less complex alternative compared to the above said methods using trigonometric functions as basis elements.

The algorithms proposed in [4], [5], [6] require more adaptive parameters i.e., in terms of the length of the nonlinear adaptive filter to be used with an increase in model order. In addition to that, RIR estimation also needs an adaptive filter with thousands of coefficients. As a result, the time needed for iteration will increase which in turn will reduce the convergence rate of NAEC [7]. The possible solution to this problem is to use a lower model order for reducing the length of nonlinear adaptive filter which will deteriorate the NAEC's ability in modelling NLD and linear adaptive filters with shorter length which will lead to under-modelling of the RIR [8].

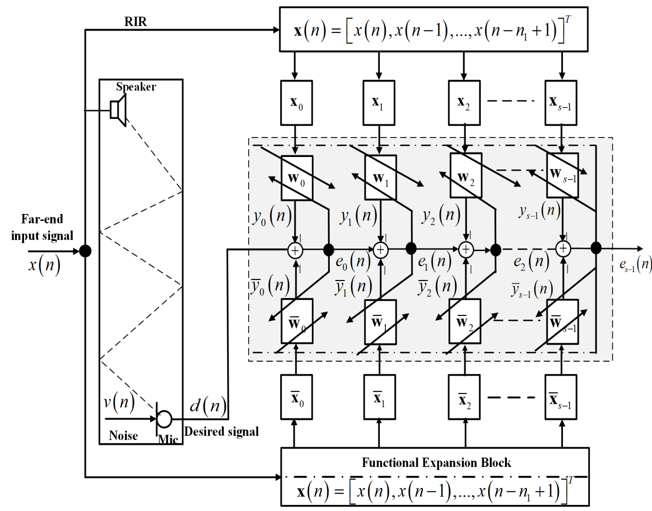

Fig. 1. Proposed nonlinear acoustic echo cancellation framework.

From these observations, it can be concluded that an NAEC with an improved convergence rate which can support in estimating the RIR with thousands of coefficients and NLD is needed.This paper intends to address this gap in the existing literature related to the requirement of an improved convergence rate while increasing the overall performance of the NAEC. In this paper we propose to address this gap with the help of an improved FL based NAEC framework. The contributions in this paper are as follows.

In this paper to increase the convergence rate of the NAEC we propose to adopt the sub-filter approach through which the linear and nonlinear filters are decomposed into a finite number of sub-filters. As a result, the computation time needed for an iteration gets reduced which will aid in improving the convergence rate.Then the sub-filters will be updated using mixed error to guarantee a better balance between convergence and steady-state performance in the resulting NAEC framework. Finally, proportionate filtering is employed to improve the convergence further.

II. Proposed Nonlinear AEC framework

Fig.1 depicts the proposed nonlinear AEC framework wherein $x(n)$ is the far-end input sample at nth time instant. The linear $\mathbf{w}_k$ and the non filtering blocks $\bar{\mathbf{w}}_k$ are fed with the $x(n)$ through the input buffer $\boldsymbol{x}(n)$ of length n_1 defined as

$$\boldsymbol{x}(n) = [x(n), x(n-1), x(n-2), ..., x(n-n_1+1)]^T. \quad (1)$$

To model the NLD in $d(n)$, the samples of $\boldsymbol{x}(n)$ will be nonlinearly expanded using functional expansion block as

$$\overline{\mathbf{x}}(n) \triangleq \left[\mathbf{a}_0\{x(n)\}, \ldots, \mathbf{a}_{n_1-1}\{x(n-n_1+1)\}\right]^T. \quad (2)$$

In Eq.(2), vector $\mathbf{a}_i\{x(n-i)\}$ (for $i \in \{0, 1, \ldots, n_1-1\}$) is an M length functional expansion of sample $x(n-i)$.

$$\boldsymbol{a}_k\{x(n-i)\} \triangleq [b_0\{x(n-i)\}, ..., b_{M-1}\{x(n-i)\}]^T, \quad (3)$$

where

$$b_j\{x(n-i)\} \triangleq \begin{cases} \sin\{k\pi x(n-i)\}, j = 2m-2, \\ \cos\{k\pi x(n-i)\}, j = 2m-1. \end{cases}$$
$$m = 1, 2, ..., M. \quad (4)$$

As a result length of $\overline{\mathbf{x}}(n)$ will be $n_2 = n_1 M$. The input buffer $\boldsymbol{x}(n)$ (resp. $\overline{\boldsymbol{x}}(n)$) of length n_1 (resp. n_2) is partitioned in s blocks, referred to as sub-filters, whose length is $n_3 = n_1/s$ (resp. $n_4 = n_2/s$). Then the response of $\boldsymbol{w}_k$ block to $\boldsymbol{x}_k(n)$ is represented as

$$y_k(n) = \boldsymbol{w}_k^T(n)\boldsymbol{x}_k(n), k = 0, 1, ..., s-1. \quad (5)$$

Similarly, the response of $\bar{\boldsymbol{w}}_k(n)$ to $\overline{\mathbf{x}}(n)$ will be

$$\bar{y}_k(n) = \bar{\boldsymbol{w}}_k^T(n)\bar{\boldsymbol{x}}_k(n), k = 0, 1, ..., s-1. \quad (6)$$

Then the error in the proposed NAEC algorithm will be derived as follows.

Case 1: The error line passing in between $\boldsymbol{w}_k(n)$ and $\bar{\mathbf{w}}_k(n)$ block represents the error in case1 expressed as

$$e_0(n) = d(n) - \boldsymbol{w}_0^T(n)\boldsymbol{x}_0(n) - \bar{\boldsymbol{w}}_0^T(n)\bar{\boldsymbol{x}}_0(n), \quad (7)$$

$$e_k(n) = e_{k-1}(n) - \boldsymbol{w}_k^T(n)\boldsymbol{x}_k(n) - \bar{\boldsymbol{w}}_k^T(n)\bar{\boldsymbol{x}}_k(n), \forall k \neq 0. \quad (8)$$

The error in the 0-th sub filtering block is calculated using the current sample of the desired signal, and the error obtained is then used to find the error in the subsequent sub-filter blocks, as shown in Fig. 1. Here, the sub-filter blocks $\boldsymbol{w}_k$ and $\bar{\boldsymbol{w}}_k$ are updated with their corresponding error signal $e_k(n)$ without waiting for error to be computed in successive blocks.

Case 2: Here, the dotted line originating from the last sub-filter error in Fig. 1, i.e., $e_{s-1}(n)$ and passing adjacent to the filter blocks, depicts the case 2 error expressed as

$$e_c(n) = d(n) - \sum_{k=0}^{s-1} \boldsymbol{w}_k^T(n)\boldsymbol{x}_k(n) + \bar{\boldsymbol{w}}_k^T(n)\bar{\boldsymbol{x}}_k(n). \quad (9)$$

The method in case 1 helps to increase the convergence rate at the cost of reduced misadjustment performance. Similarly, the case 2 method offers better misadjustment at the expense of a reduced convergence rate than case 1

$$e(n) = (1-\beta)e_k(n) + \beta e_c(n), \quad (10)$$

where the term $\beta = \log_{10}|e_k(n)/e_c(n)|, n \to \infty$ [8] referred to as the trade-off parameter helps to maintain the right balance between faster convergence offered by case 1 error and better steady-state performance of case 2 error. The sparseness in the RIR and $\bar{\boldsymbol{x}}(n)$, necessitated the use of proportionate approach in NAEC as it weighs the coefficients independently based on their magnitude [9] resulting in

$$\boldsymbol{w}_k(n+1) = \boldsymbol{w}_k(n) + \frac{\mu \boldsymbol{R}_{1k,n}\boldsymbol{x}_k(n)e(n)}{\boldsymbol{x}^T{}_k(n)\boldsymbol{R}_{1k,n}\boldsymbol{x}_k(n) + \varepsilon}, \quad (11)$$

where $k = 0, 1, ...s-1$ and ε denotes the regularization factor. The term $\boldsymbol{R}_{1k,n}$ in (11) denotes the proportionality matrix for the k-th linear block [10]

$$\boldsymbol{R}_{1k,n} = \text{diag}\{r_{1k,1}(n)\mathbf{1}_p, r_{1k,2}(n)\mathbf{1}_p, ..., r_{1k,N_1}(n)\mathbf{1}_p\}, \quad (12)$$

where $N_1 = n_3/f_1$ denotes the number of groups into which the matrix $\boldsymbol{R}_{1k,n}$ of the linear sub-filter is sub-divided, f_1 denotes the length of each group and

$$r_{1k,j}(n) = \frac{1-\alpha}{2n_3} + \frac{(1+\alpha)\|\boldsymbol{w}_j(n)\|_2}{2f_1\sum_{i=1}^{N_1}\|\boldsymbol{w}_i(n)\|_2}, j = 1, ..., N_1. \quad (13)$$

where α denotes the proportionality constant. Similarly, the weight update of nonlinear block shall be

$$\bar{\boldsymbol{w}}_k(n+1) = \bar{\boldsymbol{w}}_k(n) + \frac{\bar{\mu}\boldsymbol{R}_{2k,n}\bar{\boldsymbol{x}}_k(n)e(n)}{\bar{\boldsymbol{x}}^T{}_k(n)\boldsymbol{R}_{2k,n}\bar{\boldsymbol{x}}_k(n) + \varepsilon}, \quad (14)$$

where $k = 0, 1, ...s-1$. The term $\boldsymbol{R}_{2,k}$ denotes the proportionality matrix of the k-th block

$$\boldsymbol{R}_{2k,n} = \text{diag}\{r_{2k,1}(n)\mathbf{1}_p, r_{2k,2}(n)\mathbf{1}_p, ..., r_{2k,N_2}(n)\mathbf{1}_p\}, \quad (15)$$

where $\mathbf{1}_p$ denotes the vector of ones with length p and $N_2 = n_4/f_2$ denotes the number of groups into which the matrix $\boldsymbol{R}_{2k,n}$ of the nonlinear sub-filter is sub-divided, f_2 denotes the length of each group and

$$r_{2k,j}(n) = \frac{1-\bar{\alpha}}{2n_4} + \frac{(1+\bar{\alpha})\|\bar{\boldsymbol{w}}_j(n)\|_2}{2f_2\sum_{i=1}^{N_2}\|\bar{\boldsymbol{w}}_i(n)\|_2}, j = 1, ..., N_2 \quad (16)$$

where $\bar{\alpha}$ denotes the proportionality constant of the nonlinear filtering block. The expressions in (11) and (14) will represent the new weight update expressions in the proposed NAEC algorithm.

A. Convergence analysis

In this section, the analysis is presented with the following assumptions considering RIR to be first order Markov model:

A1. The input and the noise $\boldsymbol{x}_k(n)$, $v(n)$ are uncorrelated zero mean Gaussian random processes with variance $\sigma_{x_k}^2(n)$, $\sigma_v^2(n)$ respectively.

A2. The weight deviation vector $\boldsymbol{Q}_k(n)$ and $\boldsymbol{x}_k(n)$ are statistically independent.

The unknown echo path $d(n)$ can be expressed as [8]

$$d(n) = \boldsymbol{g}_k^T(n)\boldsymbol{x}_k(n) + v(n), \quad (17)$$

where $v(n)$ and $\boldsymbol{g}_k$ denotes the noise and the Wiener optimum solution in the k^{th} block, and

$$\boldsymbol{g}_k(n+1) = \gamma\boldsymbol{g}_k(n) + \boldsymbol{t}_k(n)\sqrt{1-\gamma^2}, \quad (18)$$

where $\boldsymbol{t}_k(n)$, $\gamma(0 < \gamma < 1)$ denotes the zero Gaussian distribution and the innovation parameter respectively. Since, the term $e_k(n) \ll e_c(n)$, the error in (10) can be modified as

$$e(n) = d(n) - \left(\sum_{k=0}^{s-1} \boldsymbol{w}_k^T(n)\,\boldsymbol{x}_k(n) + \bar{\boldsymbol{w}}_k^T(n)\,\bar{\boldsymbol{x}}_k(n)\right). \tag{19}$$

Now by substituting

$$p = \sum_{k=0}^{s-1} \bar{\boldsymbol{w}}_k^T(n)\,\bar{\boldsymbol{x}}_k(n), \tag{20}$$

and (17) in (20), the error expression becomes

$$e(n) = \boldsymbol{Q}_k^T(n)\,\boldsymbol{x}_k(n) + v(n) - p(n), \tag{21}$$

where $\boldsymbol{Q}_k(n)$ denotes the weight deviation vector. Following A2 the MSE in the proposed NAEC algorithm is

$$J = \sigma_v^2(n) + \sigma_{x_k}^2(n)\,\mathbb{E}\left[\boldsymbol{Q}_k^T(n)\boldsymbol{Q}_k(n)\right] + \sigma_p^2(n), \tag{22}$$

where $\sigma_v^2(n)$, $\sigma_{x_k}^2(n)$ and $\sigma_p^2(n)$ in (22) denote the variance of noise, input vector $\boldsymbol{x}_k(n)$ and $p(n)$, respectively. Then the weight deviation vector $\boldsymbol{Q}_k(n)$ can be updated as

$$\boldsymbol{Q}_k(n+1) = \boldsymbol{g}_k(n+1) - \boldsymbol{w}_k(n+1). \tag{23}$$

Substituting (18), (11) one can rewrite (23) in terms of individual coefficients as

$$\begin{aligned} Q_{k,l}(n+1) &= Q_{k,l}(n) + (\gamma-1)\,g_{k,l}(n) + t_{k,l}(n)\sqrt{1-\gamma^2} \\ &- \left[v(n) + \sum_{l=1}^{u} Q_{k,l}(n)x_{k,l}(n)\right]\left[\mu\frac{r_{k,l}(n)x_{k,l}(n)}{\mathbf{x}_k^T(n)\mathbf{R}_{1k,n}\mathbf{x}_k(n)+\varepsilon}\right] \\ &- p(n)\left[\mu\frac{r_{k,l}(n)x_{k,l}(n)}{\mathbf{x}_k^T(n)\mathbf{R}_{1k,n}\mathbf{x}_k(n)+\varepsilon}\right]. \end{aligned} \tag{24}$$

Taking the square of (24) along with the expectation on both sides yields

$$\begin{aligned} \mathbb{E}\left[\|\mathbf{Q}_k(n+1)\|^2\right] &= \mathbb{E}\left[\|\mathbf{Q}_k(n)\|^2\right] + 2(1-\gamma)\,\sigma_t^2(n) \\ &+ \frac{\mu^2\sigma_{x_k}^2(n)(\sigma_v^2(n)+\sigma_p^2(n))}{(\sigma_{x_k}^2+\varepsilon)^2} tr\left\{\mathbb{E}\left[\mathbf{R}_{1k}^2\right]\right\} \\ &- 2\mu\frac{\left[\left\|\mathbf{Q}_k^T(n)\mathbf{x}_k(n)\right\|^2\right] tr\{\mathbb{E}[\mathbf{R}_{1k}]\}}{(\sigma_{x_k}^2+\varepsilon)} \\ &+ \frac{\mu^2\sigma_{x_k}^2(n)}{(\sigma_{x_k}^2+\varepsilon)^2}\left[\left\|\mathbf{Q}_k^T(n)\mathbf{x}_k(n)\right\|^2\right] tr\left\{\mathbb{E}\left[\mathbf{R}_{1k}^2\right]\right\}. \end{aligned} \tag{25}$$

By replacing $\mathbb{E}\left[\left\|\boldsymbol{Q}_k^T(n)\boldsymbol{x}_k(n)\right\|^2\right]$ with ζ_k in (25)

$$\begin{aligned} \mathbb{E}\left[\|\boldsymbol{Q}_k(n+1)\|^2\right] &= \mathbb{E}\left[\|\boldsymbol{Q}_k(n)\|^2\right] + 2(1-\gamma)\,\sigma_t^2(n) \\ &+ \frac{\mu^2\sigma_{x_k}^2(n)(\sigma_v^2(n)+\sigma_p^2(n))}{(\sigma_{x_k}^2+\varepsilon)^2} tr\left\{\mathbb{E}\left[\boldsymbol{R}_{1k}^2\right]\right\} - 2\mu\frac{\mathbb{E}[\zeta_k] tr\{\mathbb{E}[\boldsymbol{R}_{1k}]\}}{(\sigma_{x_k}^2+\varepsilon)} \\ &+ \frac{\mu^2\sigma_{x_k}^2(n)}{(\sigma_{x_k}^2+\varepsilon)^2}\mathbb{E}[\zeta_k]\, tr\left\{\mathbb{E}\left[\boldsymbol{R}_{1k}^2\right]\right\}. \end{aligned} \tag{26}$$

Assuming that the algorithm converges, at steady state one has

$$\lim_{n\to\infty}\mathbb{E}\left[\|\boldsymbol{Q}_k(n+1)\|^2\right] = \mathbb{E}\left[\|\boldsymbol{Q}_k(n)\|^2\right]. \tag{27}$$

Hence, (26) gets modified as

$$\begin{aligned} &2(1-\gamma)\,\sigma_t^2(n) + \frac{\mu^2\sigma_{x_k}^2(n)(\sigma_v^2(n)+\sigma_p^2(n))}{(\sigma_{x_k}^2+\varepsilon)^2} tr\left\{\mathbb{E}\left[\boldsymbol{R}_{1k}^2\right]\right\} = \\ &\zeta_k\left(2\mu\frac{tr\{\mathbb{E}[\boldsymbol{R}_{1k}]\}}{(\sigma_{x_k}^2+\varepsilon)} - \frac{\mu^2\sigma_{x_k}^2(n)}{(\sigma_{x_k}^2+\varepsilon)^2} tr\left\{\mathbb{E}\left[\boldsymbol{R}_{1k}^2\right]\right\}\right). \end{aligned} \tag{28}$$

Simplifying (28)

$$\zeta_k = \frac{2(1-\gamma)\,\sigma_t^2(n) + \frac{\mu^2\sigma_{x_k}^2(n)(\sigma_v^2(n)+\sigma_p^2(n))}{(\sigma_{x_k}^2+\varepsilon)^2} tr\left\{\mathbb{E}\left[\boldsymbol{R}_{1k}^2\right]\right\}}{2\mu\frac{tr\{\mathbb{E}[\boldsymbol{R}_{1k}]\}}{(\sigma_{x_k}^2+\varepsilon)} - \frac{\mu^2\sigma_{x_k}^2(n)}{(\sigma_{x_k}^2+\varepsilon)^2} tr\left\{\mathbb{E}\left[\boldsymbol{R}_{1k}^2\right]\right\}}. \tag{29}$$

As $n \to \infty$ equation (29) results in a positive excess mean square error provided

$$0 < \mu < \frac{2tr\left\{\mathbb{E}\left[\boldsymbol{R}_{1k}\right]\right\}(\sigma_{x_k}^2+\varepsilon)}{\sigma_{x_k}^2(n) tr\left\{\mathbb{E}\left[\boldsymbol{R}_{1k}^2\right]\right\}}. \tag{30}$$

in ensuring the convergence of $\boldsymbol{w}_k(n)$ in the mean square sense.

III. Results & Discussion

A. Simulation setup

The performance of the proposed algorithm is validated using speech and colored noise signals as far-end input. Female speech signal sampled at 16 kHz obtained from TSP database [11] is used as far-end speech input. Similarly, the colored noise input is derived by passing white noise signal through a first order AR system given as $g(z) = \sqrt{1-\theta^2}/\left(1-\theta z^{-1}\right)$ with $\theta = 0.8$. The RIR is simulated using the method of images [12] with a sampling frequency of 16 kHz and a reverberation time of $T_{60} \approx 120$ ms with a length of 1000 samples. To simulate the NLD introduced by the loudspeakers in hands-free applications, we use the sigmoidal nonlinear function [6]

$$\bar{\boldsymbol{s}}(n) = g\left(\frac{1}{1+\exp[-ha(n)]} - \frac{1}{2}\right), \tag{31}$$

where

$$a(n) = \frac{3}{2}x(n) - \frac{3}{10}x^2(n). \tag{32}$$

and g, h are the gain and the slope. The term h is taken as

$$h = \begin{cases} 4, a(n) > 0, \\ \frac{1}{2}, a(n) \le 0 \end{cases} \tag{33}$$

The simulation parameters used are $m = 5$, $s = 4$, $\mu = 0.275$, $\bar{\mu} = 0.55$, $\varepsilon = 0.01$, $\alpha, \bar{\alpha} = 0$, $N_1, N_2 = 5$ and $f_1 = 50$, $f_2 = 500$. To measure the performance of the algorithm echo return loss enhancement (ERLE) defined as $\text{ERLE}(n) = 10\log_{10}\left\{\mathbb{E}\left[d^2(n)\right]/\mathbb{E}\left[e^2(n)\right]\right\}$, and perceptual evaluation of speech quality (PESQ) will be used as performance metrics.

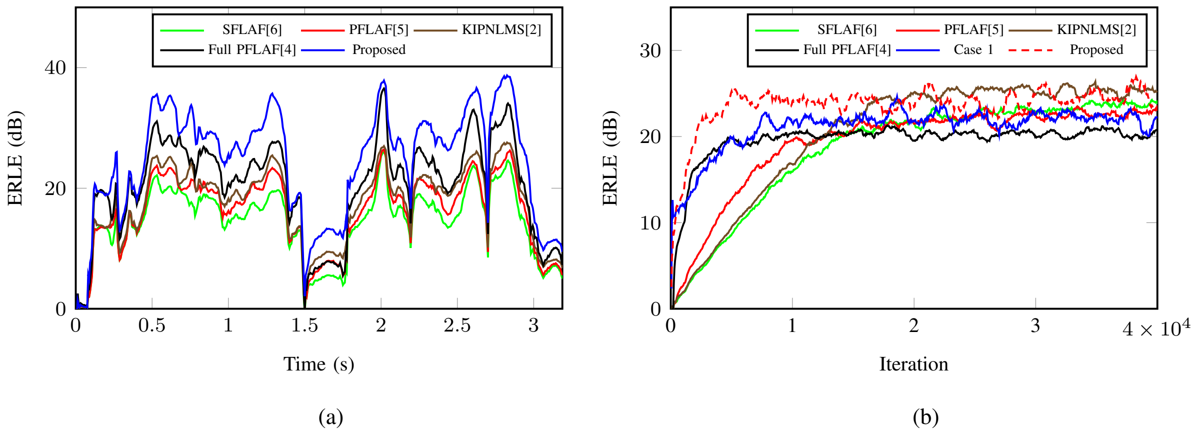

Fig. 2. ERLE performance for (a) speech input, and (b) colored noise input

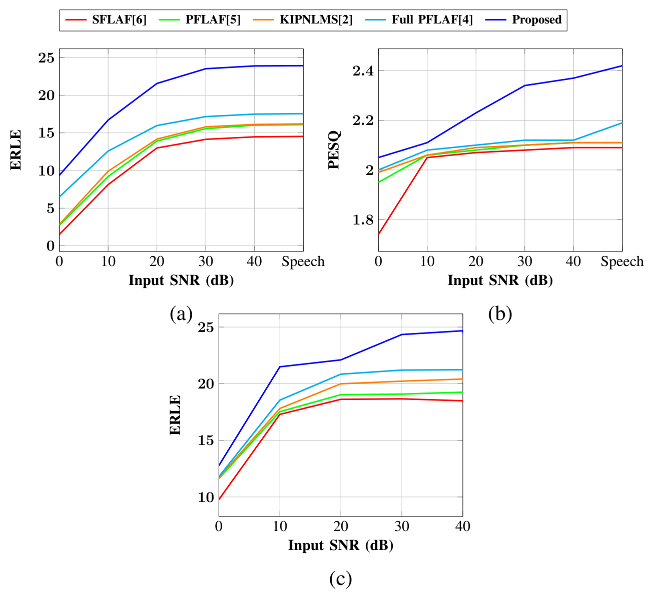

Fig. 3. (a) mean ERLE for speech input, (b) PESQ score for speech input, and (c) mean ERLE for colored noise input.

B. Speech signal input

$d(n)$ is obtained by passing speech through (31) and convolving with RIR $d(n)$. The echo component is maintained at an SNR of 30 dB using white noise. Higher ERLE is observed for the proposed NAEC compared to the existing NAEC methods suggesting the improvement in performance of the proposed NAEC. Similarly, Fig. 3(a)-3(b) depicts the ERLE and PESQ performance for speech input at different background SNR.

C. Colored noise input

Here, the desired signal is generated as mentioned in the earlier experiment for the colored noise signal. Then the white noise signal is added to it at an SNR of 30 dB. An improvement in convergence and steady-state is observed in Fig.2(a) in case of the proposed NAEC when compared with [2], [4], [5], [6] validating the enhancements brought by the proposed approach. Similarly, Fig. 3(c) depicts the mean ERLE at different background SNR values. Also comparison made between Case 1 in (7) and the proposed algorithm in Fig.3(c) validates the improvement brought by the proposed NAEC algorithm in terms of convergence and steady-state performance.

D. Computational complexity

The proposed algorithm needs $7n_1 + n_2 + 8s - 1$ multiplications and $5n_1 + n_2 + 9s - 3$ number of additions for the linear filtering block. Hence, it needs an additional amount of $n_1 + 8s - 4$ multiplications and $9s - 4$ number of additions compared to its recent functional links based NAEC counterpart Full PFLAF [4]. Similarly, the nonlinear filtering block needs $7n_2 + n_1 + 9s + n_2 s - 1$ multiplications and $5n_2 + n_1 + 10s + n_2 s - 3$ number of additions. The excess amount of computations needed is identical to the linear case. From Fig. 2 one may conclude that the additional calculations required by the proposed structure can be quite reasonable, since it obtains a significant enhancement in ERLE performance.

IV. Conclusion

In this paper, we presented a new NAEC algorithm based on sub-filter based adaptive filtering technique to improve the NAEC performance along with its convergence and steady-state analysis. The proposed approach subdivides the linear and nonlinear filter in the PFLAF algorithm into sub-filters for improving its convergence rate, which are then updated using proportionate filtering. The experimentation carried out using speech and colored inputs under simulated NLD environment have shown the improvement in the proposed algorithm over its counterparts. The work was mainly focused on improving the echo cancellation performance of NAEC in monophonic communication scenario which can be extended further to the stereophonic case as well. In addition to that, with the help of improved nonlinear modelling the performance of the NAEC can be improved further.

REFERENCES

[1] M. Schrammen, S. Kühl, S. Markovich-Golan, and P. Jax, "Efficient nonlinear acoustic echo cancellation by dual-stage multi-channel Kalman filtering," in *IEEE International Conference on Acoustics, Speech and Signal Processing (ICASSP)*, 2019, pp. 975–979.

[2] S.Sanjana, K.Asutosh, B.Srikanth, and a. V. MNS.Swamy, "Nonlinear acoustic echo cancellation with kernelized adaptive filters," *Applied Acoustics*, vol. 166, p. 107329, 2020.

[3] K. Lee, Y. Baek, and Y. Park, "Nonlinear acoustic echo cancellation using a nonlinear postprocessor with a linearly constrained affine projection algorithm," *IEEE Transactions on Circuits and Systems II: Express Briefs*, vol. 62, no. 9, pp. 881–885, 2015.

[4] D. Comminiello, M. Scarpiniti, L. A. Azpicueta-Ruiz, J. Arenas-García, and A. Uncini, "Full proportionate functional link adaptive filters for nonlinear acoustic echo cancellation," in *2017 25th European Signal Processing Conference (EUSIPCO)*, 2017, pp. 1145–1149.

[5] ——, "Nonlinear acoustic echo cancellation based on sparse functional link representations," *IEEE/ACM Transactions on Audio, Speech, and Language Processing*, vol. 22, no. 7, pp. 1172–1183, 2014.

[6] ——, "Functional link adaptive filters for nonlinear acoustic echo cancellation," *IEEE Transactions on Audio, Speech, and Language Processing*, vol. 21, no. 7, pp. 1502–1512, 2013.

[7] C.Breining, P.Dreiscitel, E.Hansler, A.Mader, B.Nitsch, H.Puder, T.Schertler, G.Schmidt, and J.Tilp, "Acoustic echo control. an application of very-high-order adaptive filters," *IEEE signal processing Magazine*, vol. 16, no. 4, pp. 42–69, 1999.

[8] K.Asutosh and MNS.Swamy, "Tap-length optimization of adaptive filters used in stereophonic acoustic echo cancellation," *Signal Processing*, vol. 131, pp. 422–433, 2017.

[9] J. V. G. de Souza, D. B. Haddad, F. da R. Henriques, and M. R. Petraglia, "Novel proportionate adaptive filters with coefficient vector reusing," *Circuits, Systems, and Signal Processing*, vol. 39, no. 5, pp. 2473–2488, Sep. 2019. [Online]. Available: https://doi.org/10.1007/s00034-019-01266-z

[10] J.Liu and S.L.Grant, "Proportionate adaptive filtering for block-sparse system identification," *IEEE/ACM Transactions on Audio, Speech, and Language Processing*, vol. 24, no. 4, pp. 623–630, 2015.

[11] P. Kabal, "TSP speech database," *McGill University, Database Version*, vol. 1, no. 0, pp. 09–02, 2002.

[12] A.Jont B and D.A.Berkley, "Image method for efficiently simulating small-room acoustics," *The Journal of the Acoustical Society of America*, vol. 65, no. 4, pp. 943–950, 1979.